The Influence of Hydrodynamic Assumptions on Ship Maneuvering

Ghalib Taimuri, Tommi Mikkola, Jerzy Matusiak, Pentti Kujala & Spyros Hirdaris
Aalto University, Mechanical Engineering (Marine Technology), Espoo,Finland
ghalib.taimuri@aalto.fi

1 Introduction

We present a preliminary assessment on the influence of the hydrodynamic assumptions associated with ship motions, for vessels maneuvering in calm waters. Three approaches are considered: (a) ***Model 1*** idealising the maneuvering of a ship in 3-dof as per Brix (1993); (b) ***Model 2*** representing the 6-dof hybrid time domain unified seakeeping / maneuvering model of Matusiak (2017); and (c) ***Model 3*** - idealising combined seakeeping and maneuvering nonlinear characteristics in 6-dof by the time domain Green function method of McTaggart (2005). Simulations of turning circle and zig-zag manoeuvers are assessed and compared against available data for two tankers (KVLCC2 & Esso Osaka) and a container ship (DTC). It is concluded that in calm waters simplified models with hydrodynamic derivatives from either RANSE CFD or model tests can be used. However, implementation of well-validated CFD hydrodynamic coefficients may be more economic for the development of practical engineering tools, such as rapid assessment tools accounting for evasiveness in ship crashworthiness (Goerlandt et al. 2012).

2 Hydrodynamic models

Over the years, maneuvering has been associated with open or restricted calm waters (i.e. in sheltered waters or in a harbor). For this reason, traditional maneuvering models assume that external actions relate with constant valued slow motion derivatives applicable at all frequencies of excitation with little or no account of ship dynamics (e.g. forward speed, heading angle, etc.). Seakeeping models assume vessel operations at a speed and heading in regular or random seas in the absence of control plane actions. They assess the influence of parasitic motions or responses of a rigid vessel to waves (e.g. Hirdaris et al., 2016). In combined seakeeping and maneuvering fluid actions that include the influence of hydrodynamic coefficients and wave environmental actions can account for operational scenarios that allow the vessel to respond in various degrees of freedom (e.g. Bailey et al., 2002 and Matusiak, 2017). From the viewpoint of operations and safety of a vessel, combining random seaway and control plane actions may be useful, especially for ships travelling with forward speed in close proximity to fixed or floating structures in severe open waters; or in shallow, restricted waters. In such cases it is possible to superimpose Froude-Krylov, diffraction, radiation and 2nd order mean forces computed from potential flow in maneuvering models that account for the influence of hull, propeller, rudder and drift forces. Hydrodynamic assumptions are from empirical formulae, CFD or model tests. Consequently, the position of the vessel during maneuvers and the associated ship speed data are transfered on seakeeping (Seo and Kim, 2011). This paper compares the following models for fine and full form vessels:

- ***Model 1*** idealises the maneuvering of a ship in calm waters by a 3-dof box-like model based on Brix (1993). The ship origin is in way of still water line and on the symmetry plane, at a distance 'x_G'(mid-ship) from the Centre of Gravity (CoG). The radiation part of the hull forces includes added mass coefficients as per Clarke et al. (1983) and Brix (1993). The mathematical equation is:

$$
\begin{aligned}
&m[\dot{u} - rv - r^2 x_G] = X_{res} + X_{prop} + X_{rud} + X_{hull} \\
&m[\dot{v} + ru + \dot{r} x_G] = Y_{rud} + Y_{Hull} \\
&(I_z + m x_G^2)\dot{r} + m[x_G(\dot{v} + ur)] = N_{rud} + N_{Hull}
\end{aligned}
\tag{1}
$$

  where : 'm' is the mass of the ship [kg] and 'I_Z' is the yaw moment of inertia; u, v and r, are surge, sway and yaw velocities respectively. Ship resistance, propulsion and rudder forces are represented with subscripts '*res*', '*prop*' and '*rud*' respectively. Subscript '*hull*' denotes hull forces.

- ***Model 2*** presents the 6-dof hybrid time domain unified model of maneuvering in waves introduced by Matusiak (2017). The ship's origin is on a line passing through CoG at still water plane and the vertical z-axis points downwards. The added mass and damping are calculated using strip theory as per Salvesen et al. (1970). Time dependent radiation forces are computed by convolution integral and hydrostatic forces are evaluated by a panel method. The mathematical equation is:

$$
\begin{aligned}
&(m+a_{11})\dot{u}+a_{15}\dot{q}=-mg\sin\theta+X_{res}+X_{prop}+X_{rud}+X_{hull}+(m+a_{22})(rv-qw)\\
&(m+a_{22})\dot{v}+a_{24}\dot{p}+a_{26}\dot{r}=mg\cos\theta\sin\varphi+(m+a_{11})(pw-ru)+Y_{hull}+Y_{rud}+a_{33}pw+a_{35}pq\\
&(m+a_{33})\dot{w}+a_{35}\dot{q}\\
&\qquad=mg\cos\theta\cos\varphi+m(uq-vp)-k_{33}-k_{35}-b_{33}w-b_{35}q+a_{11}uq+a_{15}q^2-a_{22}vp-a_{26}pr\\
&\qquad-a_{24}p^2\\
&a_{42}\dot{v}+(I_x+a_{44})\dot{p}+a_{46}\dot{r}=\left(I_y-I_z\right)qr-Y_{rud}z_{rud}+K_{hull}-k_{44}-k_{42}-k_{46}-b_{44}p+2\zeta p\omega_{\varphi}\\
&a_{15}\dot{u}+a_{53}\dot{w}+\left(I_y+a_{55}\right)\dot{q}=\left(I_y-I_x\right)pr+X_{rud}x_{rud}-k_{55}-k_{53}-k_{15}-b_{55}r-b_{35}w\\
&a_{62}\dot{v}+a_{64}\dot{p}+(I_z+a_{66})\dot{r}=\left(I_x-I_y\right)pq+Y_{rud}x_{rud}+N_{hull}
\end{aligned}
\tag{2}
$$

where: 'a_{ij}' are the added mass coefficients at infinite frequency, 'k_{ij}' is an element of memory function and 'b_{ij}' are damping radiation terms . I_x, I_y, and I_Z are roll, pitch and yaw moment of inertia respectively. Roll (φ), pitch (Θ) and heave velocities are given by p, q and w respectively; ζ *and* ω_{ϕ}, represent the critical damping ratio and angular velocity with respect to roll respectively. The hull *x*,*y* and *z* directional forces are represented by *X*, *Y* and *Z* respectively. The moments around *x*,*y* and *z* axis are denoted by *K*, *M* and *N* respectively. The remaining terms correspond, as applicable, to the same symbols as in Equation (1).

- ***Model 3*** accounts for the combined seakeeping and maneuvering characteristics of a vessel in 6-dof by a time domain green function method accounting for the nonlinearities in real hull form dynamics as per McTaggart (2005). The axis of origin is defined along North-West (X,Y).The direction of the head wave is coming from (North/X) axis (see Table 1a). The origin of the body fixed system is on CoG at a distance from still water line. At first instance hydrodynamic forces and motions are at first estimated in the frequency domain using Green function at zero forward speed. Forward speed effects are in turn implemented as a function of added mass (*[A]*) and damping (*[B]*) as per Salvesen et al. (1970). Time domain results use convolution integral and memory effects of radiation forces are determined from retardation functions embedded in (*[K]*). Incident waves and hydrostatic forces (F_{waves}) are computed non-linearly; diffracted and radiated forces are evaluated linearly and the hydrostatic restoring matrix is denoted as [*C*]. The subscripts *hull*, *prop*, *res* and *rud* show hydrodynamic, propulsion, hull-resistance and rudder forces respectively. The mathematical equation is :

$$([M]+[A])\ddot{X}+[B]\dot{X}+[C]X+[K]=F_{hull}+F_{waves}+F_{prop}+F_{res}+F_{rud} \tag{3}$$

3 Results and Discussion

Hull forces in all models include hydrodynamic derivatives estimated from empirical relations (see Table 2). For example, KVLCC2 deep-water derivatives are selected from model test results reviewed by Aksu and Köse (2017) and for shallow waters from the CFD simulations of Mucha (2017). On the other hand, Esso Osaka derivatives are opted from Kobayashi et al. (2003) model tests. DTC maneuvering coefficients use the CFD model of Kinaci et al. (2019).

Turning circle manoeuvers of KVLCC2 are shown in Figure 1(i). Results for Model 1 based on experimental and empirical derivatives show good agreement. For the same case manoeuvring trajectories produced by Models 2 & 3 deviate from experiments. Having a closer look at Model 2 it appears that the advance, transfer and tactical diameter of the ship lie within the reasonable limits of 12%, 10% and 3% respectively. The reason for these deviations may be due to the differences between the damping terms used by different methods and the coupled effects of heave, pitch and roll. In model tests and CFD models the effect of viscosity may be another term that influences hydrodynamic performance. On the other hand, in Model 3 results deviate significantly in comparison to experimental data and this could be attributed to Inoue et al. (1981) idealisation that assumes no additional surge component that would influence the resistance of the ship while progressing in way of her trajectory (see Table 2). As shown in Figure 1(ii) in a similar fashion to KVLCC2 the turning circle of Esso Osaka is close to the actual trajectory of Model 1. On the other hand, Model 2 PURE trajectory deviates significantly from the MMG and EXP trajectories, while the tactical diameter seems reasonable. It is thought that these differences appear because the higher order surge ($X'_u, X'_{uu}, X'_{uuu}, X'_v, X'_{vvv}$), sway ($Y'_{vv}, Y'_{rr}$) hydrodynamic derivatives and yaw moments (N'_{vv}, N'_{rr}) that are included in the PURE mathematical model presented in Table 2, are not incorporated in the results. This observation is also confirmed by the comparisons of results from Models 1, 2 shown in Figures 2(a),(b). It is thought that 0Model 3 results for Esso Osaka deviate in comparison to experimental data primarily for the same reasons explained for KVLCC2. For the remaining models differences may be attributed to various methods used for the derivation of hydrodynamic derivatives (see Table 2). As presented in Figure 1(iii) the DTC container ship shows satisfactory initial trajectories with Model 1 when empirical and CFD based hydrodynamic derivatives are implemented. This is not the case for Models 2 & 3 that predict adequate trajectories only for the case of CFD hydrodynamic derivatives.

Table 1. Summary of maneuvering and seakeeping Models

<table>
<tr><td colspan="3">(a) Axis of Orign (ψ: heading angle, μ : $wave\ direction$; OXY : Earth-fixed coordinate system; oxy: body coordinate system).</td></tr>
<tr><td>Model 1</td><td>Model 2</td><td>Model 3</td></tr>
<tr><td>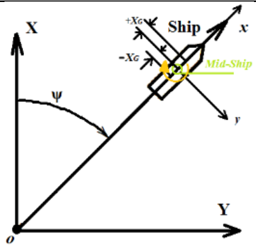
</td><td>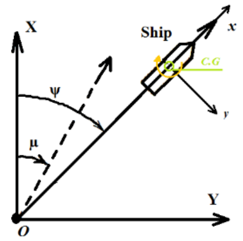
</td><td>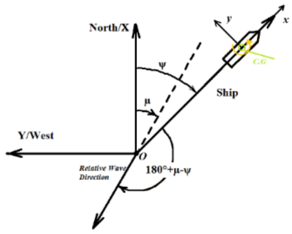
</td></tr>
<tr><td colspan="3">(b) Hull Resistance (X_{res}, F_{res})</td></tr>
<tr><td colspan="2">$X_{res} = -0.5\rho U^2 S_w C_T/(1-t)$</td><td>$F_{res} = -0.5\rho U^2 S_w C_T$</td></tr>
<tr><td colspan="3">where, X_{res}, F_{res} is hull resistance, U is the initial velocity of vessel, s_w is wetted surface area, C_T is resistance coefficient and 't' is thrust deduction factor.</td></tr>
<tr><td colspan="3">(c) Propeller Forces (X_{prop}, F_{prop})</td></tr>
<tr><td colspan="2">$X_{prop} = \rho n^2 D^4 K_T$</td><td>$F_{prop} = (1-t)\rho n^2 D^4 K_T$</td></tr>
<tr><td colspan="3">K_T is the thrust coefficient defined as: $k_{t0} + k_{t1}J + k_{t2}J^2$; where J is the advance number and $k_{t0}, k_{t1}, and\ k_{t2}$quadratic coefficients; 'D' is propeller diameter, 'n' is revolution of propeller (rps) and ρ is density of water.</td></tr>
<tr><td colspan="3">(d) Rudder Forces $(X_{rud}, Y_{rud}, N_{rud})$</td></tr>
<tr><td colspan="2">Rudder forces are estimated according to Söding, (1982), Brix, (1993)
$X_{rud} = -0.5C_D\rho A_r(V_{x,r}^2 + V_{y,r}^2)$
$Y_{rud} = 0.5C_L\rho A_r(V_{x,r}^2 + V_{y,r}^2)[0.6\cos\beta + 0.6\ X_{rud}\sin\beta]\ N_{rud} = x_R Y_{rud}$
where: C_D and C_L are rudder drag and lift coefficients'; A_r is rudder area and $V_{x,r}\ and\ V_{y,r}$ are inflow axial and radial velocity at rudder respectively; β and ρ are drift angle and density of water respectively.</td><td>Rudder forces are calculated using Inoue et al., (1981)as :
$X_{rud} = -F_N \sin\delta$
$Y_{rud} = -(1+a_H)F_N\cos\delta$
$N_{rud} = -(1+a_H)x_R\ F_N\cos\delta$
where: F_N is rudder normal force; a_H is rudder hull interaction coefficient; x_R is a distance of rudder from CoG and δ is the rudder angle.</td></tr>
</table>

Table 2. Hydrodynamic derivatives ($X_H', Y_H'\ and\ N_H'$ show linear, higher order and coupled, non-dimensional damping forces for surge force X' , sway force $Y'$and yaw moment N')

<table>
<tr><td>INOUE (Model 3) - Inoue et al., (1981)
$Y'_H = Y'_v v' + Y'_{vv}v'|v'| + Y'_{vr}v'|r'| + Y'_r r' + Y'_{rr}r'|r'|$
$N'_H = N'_v v' + N'_{vvr}v'^2 r' + N'_{vrr}v' r'^2 + N'_r r' + N'_{rr}r'|r'|$</td></tr>
<tr><td>MMG (Model 1& Model 2) - Yasukawa and Yoshimura (2015)
$X'_H = -R'_0 + X'_{vv}v'^2 + X'_{vr}v'r' + X'_{rr}r'^2 + X'_{vvvv}v'^4$
$Y'_H = Y'_v v' + Y'_r r' + Y'_{vvv}v'^3 + Y'_{vvr}v'^2 r' + Y'_{vrr}v'r'^2 + Y'_{rrr}r'^3$
$N'_H = N'_v v' + N'_{vvr}v'^2 r' + N'_{vvv}v'^3 + N'_r r' + N'_{vrr}v'r'^2 + N'_{rrr}r'^3$</td></tr>
<tr><td>PURE (Model 1 & Model 2) - Papanikolaou et al.(2016)
$X'_H = X'_v + X'_{vv}v'|v'| + X'_{vvv}v'^3 + X'_u u' + X'_{uu}u'^2 + X'_{uuu}u'^3$
$Y'_H = +Y'_v v' + Y'_{vv}v'|v'| + Y'_{vvv}v'^3 + Y'_r r' + Y'_{rr}r'|r'| + Y'_{rrr}r'^3$
$N'_H = +N'_v v' + N'_{vv}v'|v'| + N'_{vvv}v'^3 + N'_r r' + N'_{rr}r'|r'| + N'_{rrr}r'^3$</td></tr>
<tr><td>EMP (Model-1) [$X'_{vv}, X'_{vvvv}, Y'_{vvv}, Y'_{vvr}, N'_{vvv}$ Yoshimura, Masumoto, (2012), Clarke et al., (1983)], [Y'_v, N'_r, N'_v, Y'_r Clarke et al., (1983)], [Y'_{vv} Kijima, Nakiri, (1990), Inoue et al., (1981)]
$X'_H = X'_{vv}v'|v'| + +X'_{vvvv}v'^3|v'|$
$Y'_H = Y'_v v' + Y'_r r' + Y'_{vv}v'|v'| + Y'_{vvv}v'^3 + Y'_{vvr}v'|v'|r'$
$N'_H = N'_v v' + N'_{vvv}v'^3 + N'_r r'$</td></tr>
</table>

The zig-zag manoeuvers of KVLCC2 and Esso Osaka using Models 1 & 3 present satisfactory results in comparison to experimental data (see Figures 2a,b and 3b). Although the equation of PURE hydrodynamic derivatives demonstrated good results for turning circle simulations they seem less adaptable to zig-zag manoeuvres in comparison to other hydrodynamic derivative options available (see Table 2 and Models 1,2 in Figure 3). When Model 2 is used, a shift in the period of zig-zag manoeuvers becomes evident. This could be primarily attributed to the different way of modelling the effects of inertia (e.g. compare Brix, 1993 to McTaggart, 2005) and/or secondarily the effects of scaling. This matter is under further investigation. Hydrodynamic derivatives for the case of the DTC are based on the simulation of pure yawand sway and coupled yaw and sway by CFD (see Kinaci et al., 2019). Figure 2c, suggests that the most important parameter in the prediction of zig-zag manoeuvers at low speed is the 2nd order pure sway velocity force ($Y'_{vv}v'|v'|$). This is because all models presented - apart from the MMG model - take under consideration this action. This seems to lead to escalation in the overshoot angle especially at lower speeds.

For ships operating in shallow waters the forces acting on the hull, rudder and propeller are changed due to the influence of seabed, side walls and quay. As per Raven (2019) the later is believed to increase the viscous resistance of the ship, ultimately affecting the inflow induced forces to the propeller, rudder and hull. To elaborate the influence of such effects, shallow water attributes were added in the numerical code of Model 1 by considering two aspects : (1) the influence of the viscous resistance of the ship in shallow water as a function of the ship draft to sea depth (see Raven, 2019); and (2) the influence of hydrodynamic derivatives by averaging the Ankudinov et al., (1990) and Kijima and Nakiri, (1990) empirical methods. The combination of (1) and (2) is thought to provide better fit in of hydrodynamic derivatives originally derived via regression analysis. Because of lack of openly available data, only comparisons of Esso Osaka and KVLCC2 are presented in Figures 4 & 5 for sea depth / ship draft ratio of 1.2 m. The simulations for KVLCC2 (see Figure 4) utilise the CFD shallow water hydrodynamic derivatives computed of Mucha, (2017). It appears that those give good estimation for turning trajectory and zig-zag manoeuvers. On the other hand, turning circle simulations for Esso Osaka seem reliable when using the EMP and MMG models (see Figure 5). Because of lack of openly available manoeuvring trajectories and associated hydrodynamic derivatives in shallow waters, to conclude on the validity of this method further model tests, open water tests and / or CFD simulations have to be pursued.

(a) Model 1 (b) Model 2 (c) Model 3

(i) KVLCC2 Tanker ship (Speed : 15.5 Knots, Rudder angle : 35^0 portside turn)

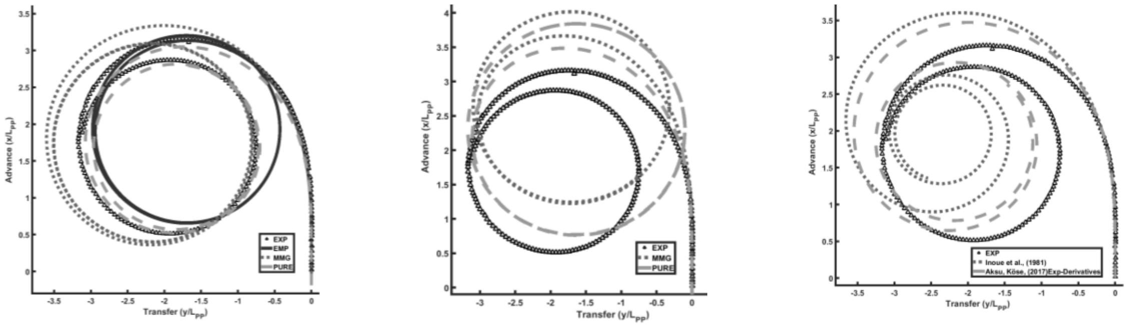

(ii) Esso Osaka Tanker ship (Speed : 10 knots, Rudder angle : 35^0 starboard turn)

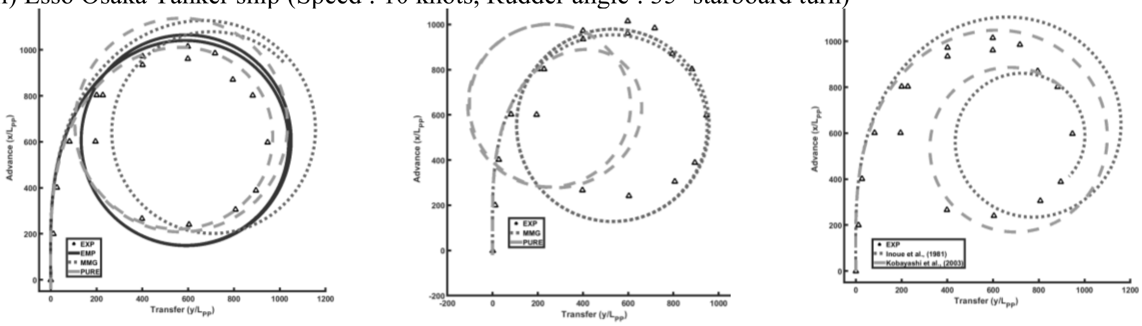

(iii) DTC Container ship (Speed : 6 knots, Rudder angle : 35^0 starboard turn)

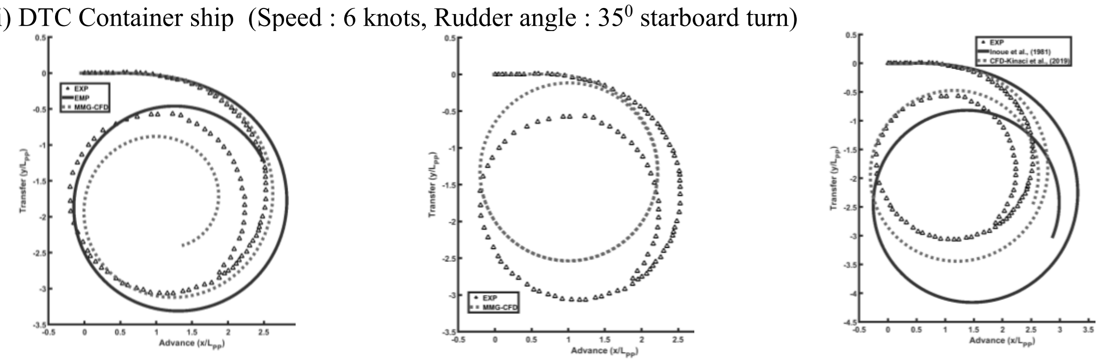

Fig. 1: Deep water turning circle simulations for all ships. (EXP denotes results from model tests; EMP & Inoue et al.,1981 represent the hydrodynamic coefficients of Table 2. For KVLCC2 and Esso Osaka the hydrodynamic derivatives are from Aksu and Köse (2017) and model tests of Kobayashi et al. (2003) respectively. DTC hydrodynamic derivatives are based on CFD by Kinaci et al.,2019).

(a) Esso Osaka (Speed :7.8 knots) (b) KVLCC2 (Speed : 15.5 knots) (c) DTC (Speed : 6 knots)

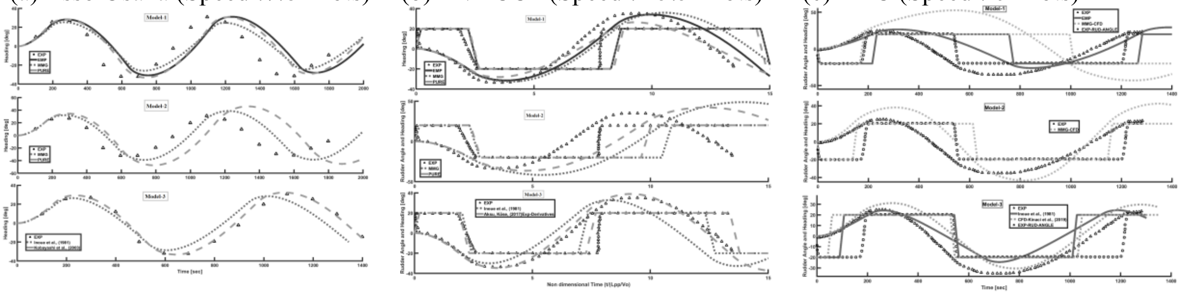

Fig. 2: Comparison of deep water $20^0/20^0$ zig-zag manoeuvres (EXP are model test results; for other hydrodynamic derivatives see Table 2 and Figure 1).

(a) Turning circle (b) Zig-zag

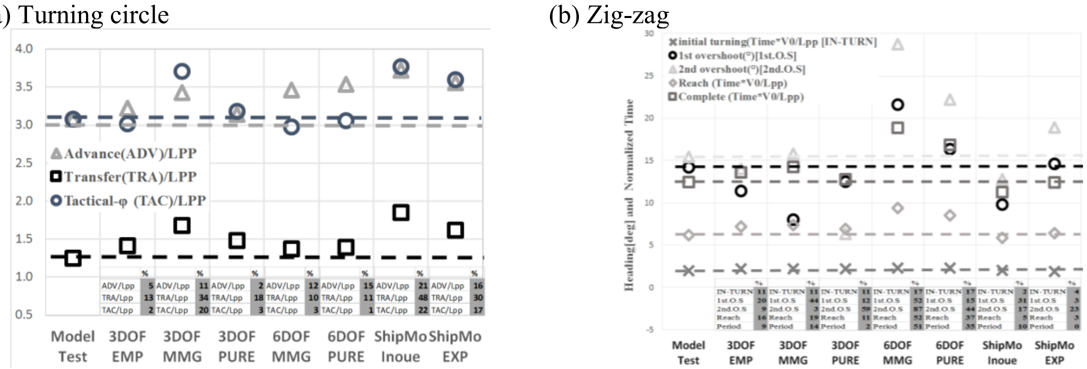

Fig. 3: Parametric study of deep water KVLCC2 manoeuvring simulations (LPP : Length between perpendiculars; V_0 : initial ship speed; for other hydrodynamic derivatives see Table 2 and Figure 1).

(a)Turning circle manouvers Rudder angle : 35^0 portside turn (b) $20^0/5^0$ Zig-zag manouvers

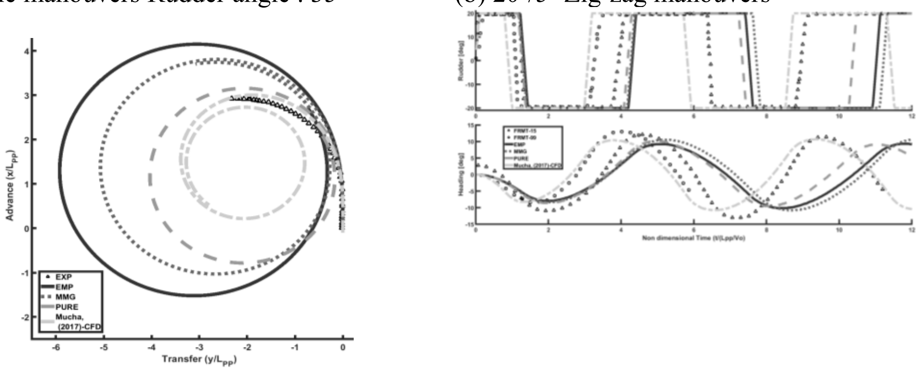

Fig. 4: Shallow water simulations for KVLCC2 using Model 1 at 7.5 Knots (EXP denotes model test results; for other hydrodynamic derivatives see Table 2 – FRMT-15 and FRMT – 99 represent free running model tests from two facilities under http://simman2019.kr .

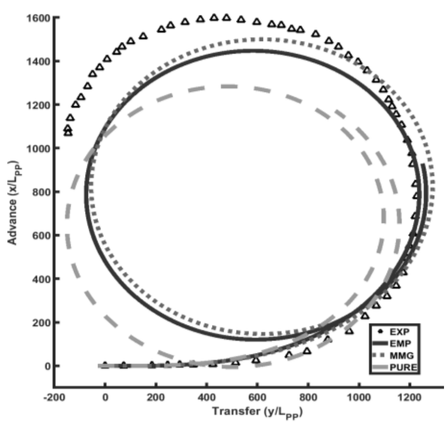

Fig 5: Shallow water manoeuvring simulation for turning circle of Esso Osaka at 7 knots speed and 35° portside turn; EXP denotes results from full-scale trials. For other hydrodynamic derivatives see Table 2. EMP represents empirically evaluated hydrodynamic coefficients, other hydrodynamic derivatives are based on model test which are converted into shallow water using empirical realtion by Ankudinov et al. (1990) and Kijima and Nakiri (1990).

4 Conclusions

- In shallow waters EMP and MMG models were shown to be suitable for Esso Osaka as compared to full-scale data. For KVLCC2 viscous effects in model experiments tend to overestimate full-scale results.
- Pure sway velocity force ($Y'_{vv}v'|v'|$) was shown to be particularly important for zig-zag manoeuvers. Differences in zig-zag test results could be attributed to uncertainties associated with added mass formulations. This could be particularly important in terms of idealising the maneuvering trajectories of vessels with standard propulsion set up (singe screw) as demonstrated in this paper, or more innovative propulsion configurations (e.g. RoPax and passenger vessels with podded or twin-screw propulsion).
- In shallow waters transforming deep-water hydrodynamic coefficients by empirical relations seems to be the traditional practice. However, validated CFD based hydrodynamic derivatives exist in open literature and depending on the case could be practically implemented in numerical codes.
- The 3-dof simplified manoeuvring model (Model 1) appears to give better results. This is encouraging, as our intention is to use this model or a more intelligent derivative of the same including wind effects and roll motions to idealise ship state before possible grounding or collision. In such situations the trajectory and speed are key parameters in terms of rounding up the influence of hydrodynamic actions on dynamic response. Model tests are expensive and the uncertainties associated with the estimation of maneuvering coefficients especially in restricted and / or shallow waters may be significant. In this sense well validated CFD simulations available in open literature could be useful.

References

Aksu, E. & Köse, E. (2017). Evaluation of Mathematical Models for Tankers' Maneuvering Motions, *Journal of ETA Maritime Science,* 5(1):95-109.

Ankudinov, V.K., Miller, E.R., Jakobsen, B.K. & Daggett, L.L. (1990). Maneuvering performance of tug/barge assemblies in restricted waterways, *Proc. of the Intl. Conference on Marine Simulations and Ship Maneuverability (MARSIM),* pp. 311 - 319, Tokyo, Japan, 4-7 June 1990.

Bailey, P.A., Hudson, D.A., Price, W.G. & Temarel, P. (2002). Time simulation of maneuvering and seakeeping assessments using a unified mathematical model, *Trans. of the Royal Inst. of Nav. Archs.,* 144: 27-48.

Brix, J.E. 1993, *Manoeuvring technical manual,* Seehafen Verlag.

Clarke, D.P., Gedling, P. & Hine, G. (1983). *The Application of Manoeuvring Criteria in Hull Design Using Linear Theory. In Maritime Archives of the the Royal Inst. of Nav. Archs.,* Report 03-1983.

Goerlandt, F., Ståhlberg, K. & Kujala, P. (2012). Influence of impact scenario models on collision risk analysis, *Ocean Engineering,* 47:74-87.

Hirdaris, S.E., Lee, Y., Mortola, G., Incecik, A., Turan, O., Hong, S.Y., Kim, B.W., Kim, K.H., Bennett, S., Miao, S.H., Temarel, P. (2016). The influence of nonlinearities on the symmetric hydrodynamic response of a 10,000 TEU Container ship, Ocean Engineering, 111:166-178.

Inoue, S., Hirano, M., Kijima, K. & Takashina, J. (1981). A practical calculation method of ship maneuvering motion, *International Shipbuilding Progress,* 28:207-222.

Kijima, K. & Nakiri, Y. (1990). Prediction method of ship manoeuvrability in deep and shallow waters,. *Proceedings of the Intl. Conference, Marine Simulation and Ship Manoeuvrability (MARSIM & ICMS)*, vol. 90, pp. 311-319, Tokyo, Japan, 4-7 June 1990.

Kinaci, O.K., Sukas, O.F. & Bal, S. (2019). A modular mathematical approach to predict the maneuvering ability of the Duisburg test case in regular waves, *Proceedings of the 5th Ship Manoeuvring in Shallow and Confined Water with non-exclusive focus on manoeuvring in waves, wind and current (MASHCON)*, pp. 251-264, 19 - 23 May 2019, Ostend, Belgium.

Kobayashi, H, Blok, J J, Barr, R, Kim, Y S and Nowicki, J. (2003). *Specialist Committee on Esso Osaka: Final Report and Recommendations to the 23rd ITTC,* vol. 2, pp. 581–743.

Matusiak, J. (2017). *Dynamics of a rigid ship,* 2nd Edition, Aalto University Series, Helsinki, Finland.

McTaggart, K. (2005). Simulation of Hydrodynamic Forces and Motions for a Freely Maneuvering Ship in a Seaway, *Defense R&D Canada (DRDC - Atlantic) Technical Memorandum,* TM:2005-071.

Raven, H.C. (2019). Shallow water effects in ship model testing and at full scale, *Technical Report of the Knowledge Centre for Maneuvering in Shallow and Confined Water*, Maritime Technology Division, Ghent University and Flanders Hydraulics Research, Belgium.

Seo, M. & Kim, Y. (2011). Numerical analysis on ship maneuvering coupled with ship motion in waves, *Ocean Engineering,* 38(17-18):1934-1945.

Söding, H. (1982). Prediction of ship steering capabilities, *Schiffstechnik,* 29(1):3-29.

Yoshimura, Y. & Masumoto, Y. (2012). Hydrodynamic database and maneuvering prediction method with medium high-speed merchant ships and fishing vessels, *Proceedings of the Intl. Conference on Marine Simulations and Ship Maneuverability (MARSIM),* pp. 494-503, 23-27 April 2012, Singapore.